


Structure of Parallel Mechanism Combined with Waterbomb-Base-Inspired Origami [†]

Lulu Al Marjan and Shyh-Chour Huang * 

Department of Mechanical Engineering, National Kaohsiung University of Science and Technology, Kaohsiung 807618, Taiwan; fl09142190@nkust.edu.tw

* Correspondence: shuang@nkust.edu.tw

[†] Presented at the 3rd IEEE International Conference on Electronic Communications, Internet of Things and Big Data Conference 2023, Taichung, Taiwan, 14–16 April 2023.

Abstract: Structure from the geometry and analysis of the three-spherical kinematic chain-base parallel mechanism have been studied. The parallel mechanism evolved from an origami fold as chain legs with three spherical kinematic chains becoming rigid bodies. The parallel mechanism with a three 6R kinematic chain as three chain legs is complicated. The reconfiguration of the parallel mechanism with full tilt–circle movement, kinematic, and workspace are investigated, too. This parallel mechanism can be applied in specific applications with certain treatments.

Keywords: origami inspires; parallel mechanism; spherical mechanism

1. Introduction

The parallel mechanism is the system that converts the motions of several bodies into constrained motions of other bodies [1]. The parallel mechanism has a closed-loop as a type of mechanism [1], and that is made of an end-effector (mobile platform) [2] and a fixed platform, linked together by independent kinematic chains [1]. Furthermore, structure, workspace considerations, singularities, and link interference need to be considered in the design [2]. The parallel mechanism has much potential in several fields, including industrial, space, medical science, and miscellaneous applications [2].

Origami is Japanese cultural art, which is the art of folding paper. In general, origami starts with flat paper (2D object), then folds become a 3D object with various shapes and forms without stretching, cutting, or gluing [3]. Moreover, origami has become an inspiration for engineers in various fields. Especially waterbomb-base origami has become an inspiration in engineering for several applications. Fonseca and Savi [3] presented an investigation of the origami waterbomb-base pattern from its unit cell and explored the different formulations for origami structure. Liang, Gao, Huang, and Li [4] presented the design of a pneumatic rigid–flexible coupling origami gripper from a waterbomb-base origami pattern. Salerno, Zhang, Menciassi, and Dai [5] proposed the concept of a miniaturized surgical tool grasper as a 3-DOF parallel module inspired by the waterbomb-base origami.

It is common to see the creases of origami mechanisms as the compliant mechanism joint with flexible material. However, the origami mechanism becomes rigid if the creases are replaced with non-flexible material. One of the rigid kinematic origami models describes the creases with the revolute joint mechanism [6].

2. Geometry of Parallel Mechanism

A parallel mechanism consists of a base, a platform, and legs to sustain the platform. The leg structure is obtained from waterbomb-base origami, which involves the spherical kinematic chain with a close loop structure. The parallel mechanism consists of three legs and one actuator in the middle of the mechanism.



Citation: Al Marjan, L.; Huang, S.-C. Structure of Parallel Mechanism Combined with Waterbomb-Base-Inspired Origami. *Eng. Proc.* **2023**, *38*, 51. <https://doi.org/10.3390/engproc2023038051>

Academic Editors: Teen-Hang Meen, Hsin-Hung Lin and Cheng-Fu Yang

Published: 26 June 2023



Copyright: © 2023 by the authors. Licensee MDPI, Basel, Switzerland. This article is an open access article distributed under the terms and conditions of the Creative Commons Attribution (CC BY) license (<https://creativecommons.org/licenses/by/4.0/>).

2.1. Waterbomb-Base Origami for Spherical Mechanisms

As shown in Figure 1a,b, origami starts with flat paper and then folds to become creases. The creases consist of two types. The first type has a convex shape called Mountain creases, denoted by M, and the second type has a concave shape called Valley creases, represented by V [7,8].

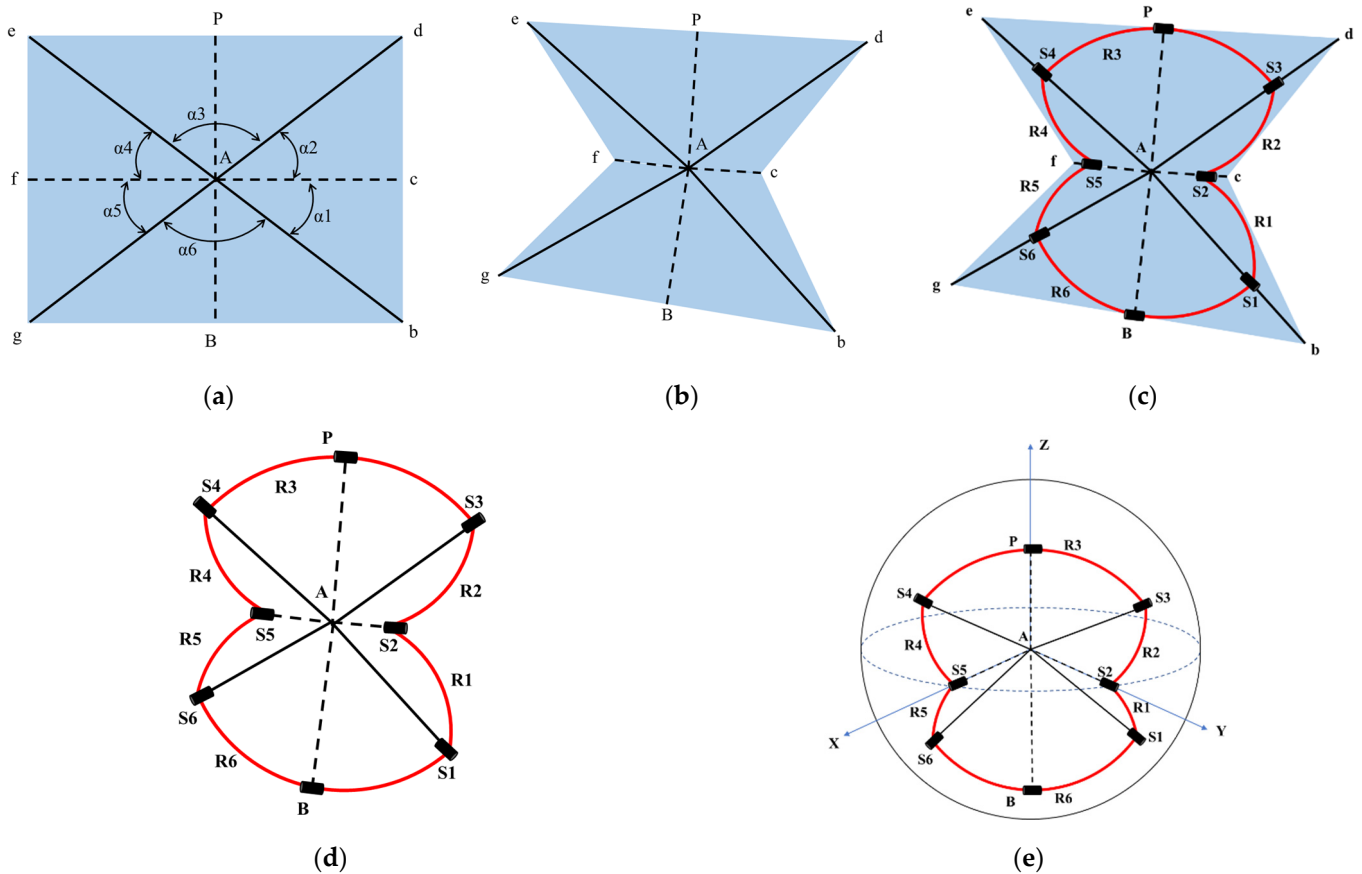


Figure 1. Waterbomb-base origami involves a spherical mechanism. (a) origami starts with flat paper; (b) origami starts fold become a crease; (c) the creases and the planes on the waterbomb-base structure; (d) the figure mapping the spherical mechanism from the origami evolved; (e) the spherical mechanism.

Waterbomb-base origami consists of six planes and six creases. Of the six creases, Ac and Af are the valley-crease types, and Ab, Ad, Ae, and Ag are the mountain-crease types. As shown in Figure 1c, the creases and the planes on the waterbomb-base structure are represented for the revolute pairs and the links, respectively [7]. Thus, the waterbomb-base origami form contains six revolute pairs and six links. Barreto et al. [8] made an analogy between the spherical mechanism and the origami vertex as a concept of mechanism design.

Maekawa’s-Justin’s Theorem [9] is as follows. Let M be the number of mountain creases and V be the number of valley creases adjacent to a vertex in a flat origami crease pattern. Then, $M - V = \pm 2$. Moreover, Kawasaki–Justin’s Theorem [9] lets v be a vertex of degree 2n is an origami crease pattern and $\alpha_1 \dots, \alpha_{2n}$ be the consecutive angles between the creases. Then, the creases adjacent to v (locally) fold flat only if

$$\alpha_1 - \alpha_2 + \alpha_3 - \dots - \alpha_{2n} = 0 \tag{1}$$

That is, the two theorems correspond with waterbomb-base origami form. As shown in Figure 1d,e, the figure mapping and the spherical mechanism from the origami evolve. In the waterbomb base origami, Point A is the intersection of the whole of the connected

creases, while in the spherical mechanism, point A is the virtual point intersection of the axis from the whole revolute pair in the spherical kinematic chain. The revolute pair and links are denoted with S and R , respectively. The link R_i ($i = 1, 2, \dots, 6$) is deformed by revolute joints S_{i-1} and S_i . Due to this close loop structure, link R_6 forms by revolute joint S_6 and S_1 . R_3 and R_6 have a revolute joint for connecting mobile and base platforms. Link R_i ($i = 1, 2, \dots, 6$) has the angle α_i ($i = 1, 2, \dots, 6$). The relationship between the angles in waterbomb-base origami is $\alpha_1 = \alpha_2 = \alpha_4 = \alpha_5$; meanwhile, $\alpha_3 = \alpha_6$.

The initial shape of waterbomb-base origami can be a square ($bd = de$) or a rectangular ($bd < de$), depending on the intended use, application, and other parameters. Determining it requires further discussion.

2.2. Parallel Mechanism

The parallel structure mechanism consists of a mobile platform, a fixed platform, three legs, and a truss in the middle of the mechanism. Meanwhile, the legs are represented by the spherical kinematic chain involved in waterbomb-base origami, and then, the structure has three spherical kinematic chains for the legs [7]. The truss consists of a prismatic connector hinge and two offset universal hinges to connect to the mobile platform and base platform. The truss component has supported the movement of the mobile platform concerning the base platform.

Figure 2 shows the revolute pair S_{ij} and the link R_{ij} , where i ($i = 1, 2, 3$) is the number of legs and j ($j = 1, 2, \dots, 6$) is the number of a revolute pair. P and B are the revolute joints paired with the mobile and base platforms.

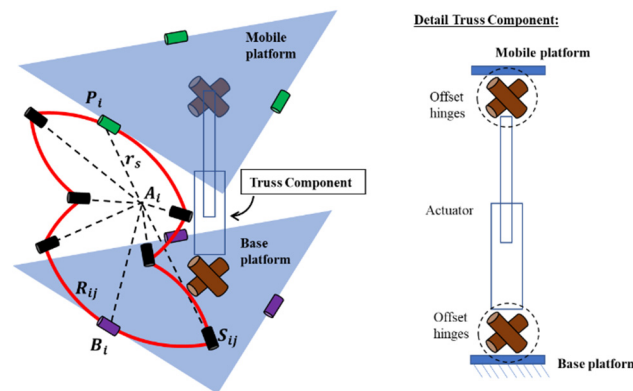


Figure 2. Structure of parallel mechanism.

3. Kinematic of Structure Mechanism

In this section, the displacement analysis of the parallel mechanism is presented. This parallel mechanism establishes global reference and local reference. Point O_b -XYZ is established as the global reference frame at the base platform. The X-axis and the Y-axis are perpendicular and parallel to the axis of the revolute hinge with the center point B_1 , respectively. At the same time, the Z-axis is normal to the base following the right-hand rule [7]. In addition, the mobile platform has a point O_p -XYZ as the midpoint, and the legs and the truss component have the local reference frame. Table 1 explains the procedure of the DH Convention for knowing the forward kinematics [10].

The table presents the DH parameter determined by four transformation parameters [10] from the link and joint parameters [11]. Link parameters are the length of the link (a_i) and the angle of a twist of a link (α_i); meanwhile, joint parameters as the offset of link (d_i) and joint angle (θ_i) represent the relative positions of the following links [11].

Table 1. Table of Procedure based on DH Convention.

Step 1	Determining and labeling of the joint axis Z_0, \dots, Z_{n-1} .
Step 2	Determine the base frame. Set the origin on Z_0 -axis. X_0 -axis and Y_0 -axis are chosen conveniently, according to the right-hand rule frame. For $i = 1, \dots, n - 1$
Step 3	The origin is O_i , where the common is normal to Z_i and intersects between Z_{i-1} and Z_i . If Z_i intersects with Z_{i-1} , then the O_i is located at that intersection, or if Z_i and Z_{i-1} are parallel, the origin O_i is located in any convenient position along Z_i .
Step 4	Determine the X_i from the origin O_i along the common normal between Z_{i-1} and Z_i , or if Z_{i-1} and Z_i intersects, the direction normal to the $Z_{i-1} - Z_i$ plane.
Step 5	Determine Y_i to complete the frame according to the right-hand rule.
Step 6	Determine the end-effector frame $O_n - X_n Y_n Z_n$. Define the origin O_n along Z_n , preferably at the center of the end-effector, and set X_n and Y_n following the right-hand rule.
Step 7	Create a table of DH parameters.
Step 8	Substituting the DH parameters into the equation to obtain the form of the homogeneous transformation matrices.
Step 9	The product result from step 8 is then given the position and orientation of the end-effector with respect base coordinate frame.

In Ref. [10],

- a_i = distance from the intersection of the x_i , and z_{i-1} -axis to point O_i are measured along x_i ;
- α_i = angle from z_{i-1} to z_i is measured about x_i .
- d_i = distance from O_{i-1} to the intersection of the x_i and z_{i-1} -axis are measured along z_{i-1} . If joint i is prismatic, d_i is variable.
- θ_i = angle from x_{i-1} to x_i , and is measured about z_{i-1} . If joint i is revolute, θ_i i is variable.

3.1. Leg

In Ref. [3], the waterbomb chain is related to a close chain, and the last revolute joint pairs with the first revolute joint. Therefore, waterbomb chain does not have an end effector. In this regard, evaluating the close loop equation is necessary, rather than considering the end-effector [3].

3.2. Truss Parallel Mechanism

The truss component section consists of a prismatic hinge connector, and two offset universal hinges connect to the mobile platform and the base platform. Figure 2 shows the detail of the truss component. Point O_6 and point O_1 are the center of the hinge axe connected to the mobile platform and the base platform, respectively. Point O_2 and point O_5 are the centers of the two universal hinge axes. At the same time, point O_5 and point O_4 are directly connected to the prismatic hinge [12]. l represents the prismatic hinge length, the distance between the center point O_3 and point O_4 . Each hinge axe variable has the offset distance between the center of the local coordinate hinge axe. The distance between point O_b and point O_p represents the height of the mechanism (h).

Table 1 shows the procedure of the DH convention. As shown in Figure 3, the axis of each joint is already available, which corresponds from step 1 to step 7. Table 2 shows the Denavit–Hartenberg (DH) parameters [13] of the truss component for each link.

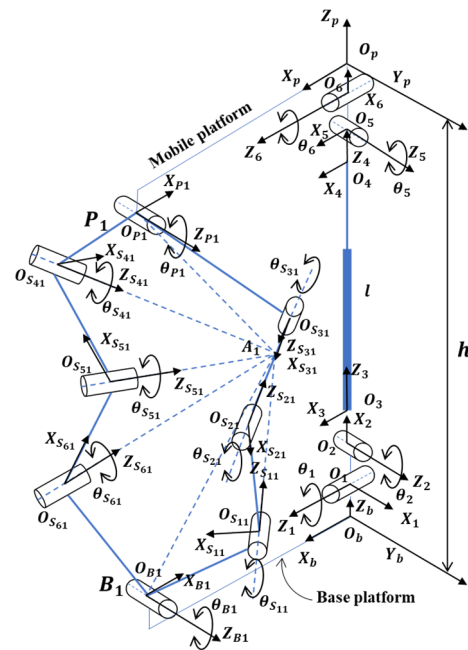


Figure 3. Kinematic model with global coordinate frame and local coordinate frame.

Table 2. Denavit–Hartenberg (DH) parameter of the truss component.

Link <i>i</i>	a_i	α_i	d_i	θ_i
1	0	90	d_1	$90 + \theta_1$
2	a_2	90	0	$90 + \theta_2$
3	0	90	d_3	90
4	0	90	d_4	θ_4
5	a_5	90	0	$90 + \theta_5$
6	0	90	0	90

According to step 8 in Table 1, substituting Equation (3) obtains the form of the homogeneous transformation matrices.

$$T_i^{i-1} = T_{Rz}(\theta).T_z(d).T_{Rx}(\alpha).T_x(a) \tag{2}$$

$$T_i^{i-1} = \begin{bmatrix} c\theta & -s\theta.c\alpha & s\theta.s\alpha & a.c\theta \\ s\theta & c\theta.c\alpha & -c\theta.s\alpha & a.s\theta \\ 0 & s\alpha & c\alpha & d \\ 0 & 0 & 0 & 1 \end{bmatrix} \tag{3}$$

$$T_0^6 = \prod_{i=1}^6 T_i^{i-1} \tag{4}$$

$$T_0^6 = T_0^1.T_1^2.T_2^3.T_3^4.T_4^5.T_5^6 \tag{5}$$

Equation (5) gives the position and orientation of the mobile platform with respect base platform, as shown in Figure 4.

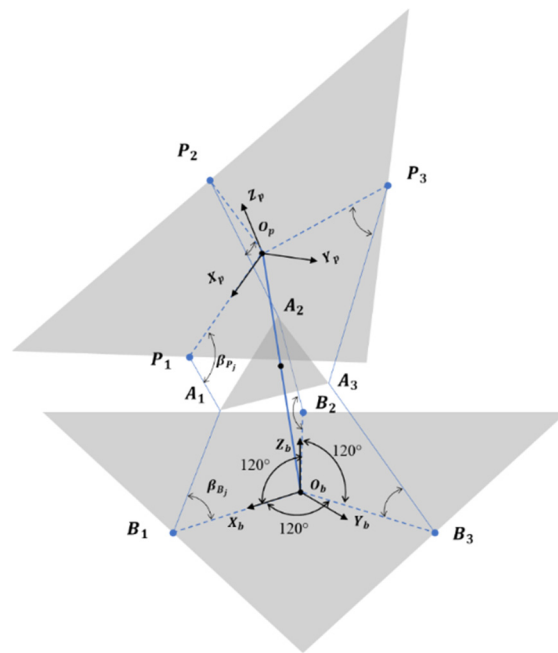


Figure 4. Schematic of the parallel mechanism.

4. Motion Characteristics of a Structure Mechanism

In this structure, the truss component is active, and the legs are passive. Therefore, the active component moves as the structure drives, while the passive component limits the driven movement.

4.1. Rotation around X-axis

Figure 5 shows the rotation around the X-axis of the global coordinate frame in the base platform. The rotation happens due to the rotation of the Z₁-axis. The rotation of the Z₆-axis determines the orientation of the end effector. The revolute hinge rotates clockwise or counterclockwise. Activating the prismatic hinge adjusts the radius of the structure’s rotation. The minimum and maximum radii are the prismatic hinge’s minimum and maximum strokes, respectively.

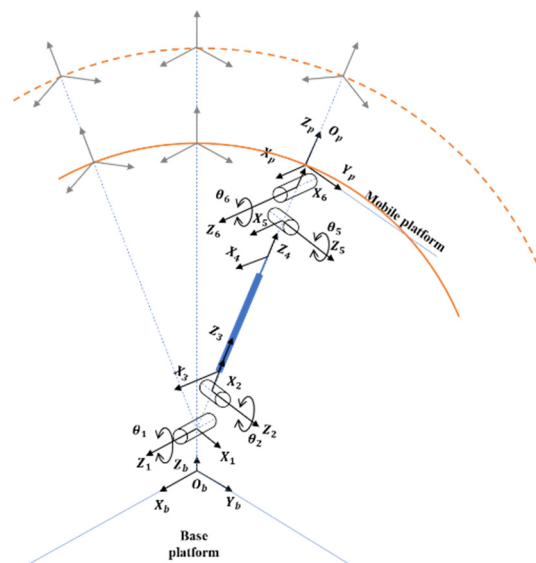


Figure 5. Rotation around the X-axis.

4.2. Rotation around Y-axis

Figure 6 shows the rotation around the Y-axis of the global coordinate frame in the base platform. The rotation happens due to the rotation of the Z_2 -axis. The rotation of the Z_5 -axis determines the orientation of the end effector. The revolute hinge rotates clockwise or counterclockwise. Activating the prismatic hinge adjusts the radius of the structure's rotation. The minimum and maximum radii are the prismatic hinge's minimum and maximum strokes, respectively.

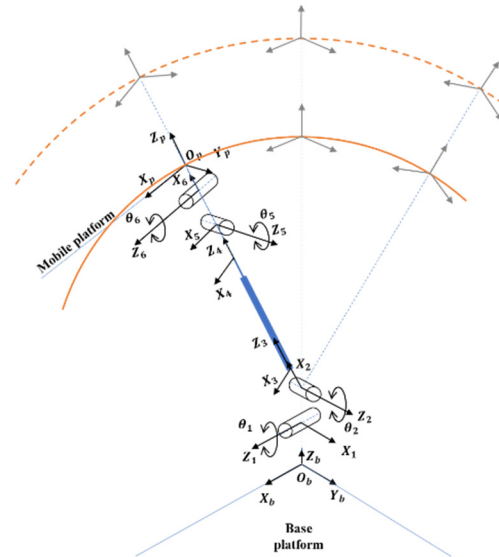


Figure 6. Rotation about the Y-axis.

4.3. Translation along X-axis

Figure 7 shows the translation along the X-axis of the global coordinate frame in the base platform. The translation movement activates the combination of two rotations and a prismatic hinge. Meanwhile, the rotations occur on the Z_2 -axis and the Z_5 -axis. The translational moving away depends on the stroke of a prismatic hinge. Furthermore, the angle degree of the Z_2 -axis is the same as with the Z_5 -axis in the opposite direction. Thus, the rotation on the revolute hinge can rotate clockwise or counter-clockwise.

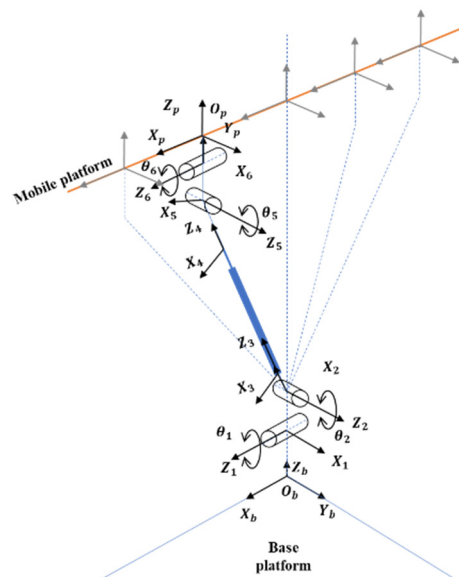


Figure 7. Translation along the X-axis.

4.4. Translation along Y-axis

Figure 8 shows the translation along the Y-axis of the global coordinate frame in the base platform. The translation movement activates the combination of two rotations and a prismatic hinge. Meanwhile, the rotation happens on the Z_1 -axis and the Z_6 -axis. The translational moving away depends on the stroke of a prismatic hinge. Moreover, the angle degree of the Z_1 -axis is the same as with the Z_6 -axis in the opposite direction. Thus, the revolute hinge rotates clockwise or counterclockwise.

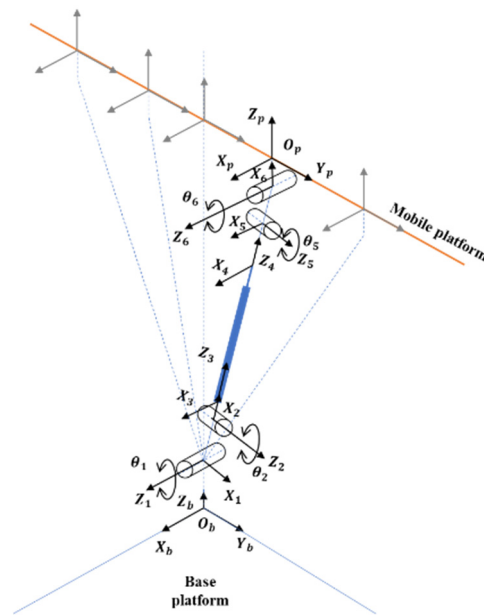


Figure 8. Translation along the Y-axis.

4.5. Translation along Z-axis

Figure 9 shows the translation along the Z-axis of the global coordinate frame in the base platform. The translation movement only activates a prismatic hinge. The high of the structure's parallel mechanism depends on the stroke of the prismatic joint.

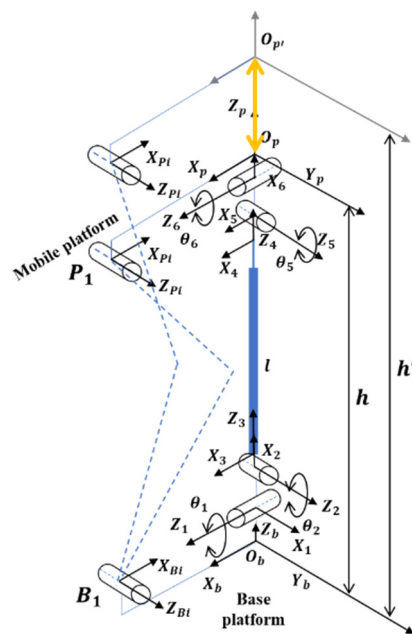


Figure 9. Translation along the Z-axis.

4.6. Rotation with Tilt Movement

As shown in Figure 10, there is a combination of the structure movement parallel mechanism. The mechanism shows a tilt with moving around. All motors can be active and need control, depending on the requirements.

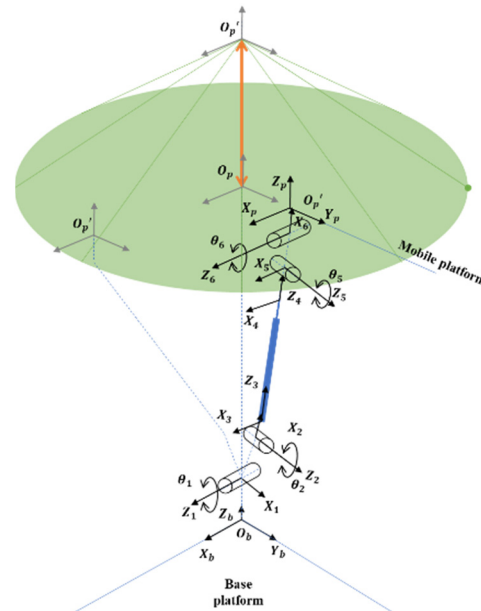


Figure 10. Rotation with tilt movement.

5. Conclusions

The parallel structure mechanism consists of a mobile platform, a fixed platform, three legs, and a truss in the middle of the mechanism. Point O_b -XYZ is established as the global reference frame at the base platform. Movement of the structure to the O_b -XYZ is observed in the base platform. There are six motion characteristics of the structure mechanism.

Author Contributions: Conceptualization, S.-C.H.; methodology, L.A.M. and S.-C.H.; software, L.A.M.; validation, S.-C.H.; formal analysis, L.A.M.; investigation, S.-C.H.; writing—original draft preparation, L.A.M.; writing—review and editing, S.-C.H.; project administration, S.-C.H. All authors have read and agreed to the published version of the manuscript.

Funding: This research received no external funding.

Institutional Review Board Statement: Not applicable.

Informed Consent Statement: Not applicable.

Data Availability Statement: Not applicable.

Acknowledgments: The authors acknowledge and thank the Ministry of Science and Technology of the Republic of China for their partial financial support of this study under Contract Number MOST 111-2221-E-992-068.

Conflicts of Interest: The authors declare no conflict of interest.

References

1. Liu, X.; Wang, J. Classification of Parallel Mechanisms. In *Parallel Kinematics*; Springer: Berlin/Heidelberg, Germany, 2014; pp. 3–29.
2. Patel, Y.D.; George, P.M. Parallel Manipulators Applications—A Survey. *Mod. Mech. Eng.* **2012**, *2*, 57–64. [[CrossRef](#)]
3. Fonseca, L.M.; Savi, M.A. On the symmetries of the origami waterbomb pattern: Kinematics and mechanical investigations. *Meccanica* **2021**, *56*, 2575–2598. [[CrossRef](#)]
4. Liang, D.; Gao, Y.; Huang, H.; Li, B. Design of a Rigid-Flexible Coupling Origami Gripper. In Proceedings of the 2021 IEEE International Conference on Robotics and Biomimetics (ROBIO), Sanya, China, 27–31 December 2021; pp. 1283–1287. [[CrossRef](#)]

5. Salerno, M.; Zhang, K.; Menciassi, A.; Dai, J.S. A Novel 4-DOF Origami Grasper with an SMA-Actuation System for Minimally Invasive Surgery. *IEEE Trans. Robot.* **2016**, *32*, 484–498. [[CrossRef](#)]
6. Bowen, L.A. A Study of Action Origami as Systems of Spherical Mechanisms. Ph.D. Thesis, Brigham Young University, Provo, UT, USA, 2013.
7. Zhang, K.; Fang, Y.; Fang, H.; Dai, J. Geometry and Constraint Analysis of the Three-Spherical Kinematic Chain Based Parallel Mechanism. *J. Mech. Robot.* **2010**, *2*, 031014. [[CrossRef](#)]
8. Barreto, R.L.P.; Morlin, F.V.; Souza, M.B.D.; Carboni, A.P.; Martins, D. Multiloop origami inspired spherical mechanisms. *Mech. Mach. Theory* **2021**, *155*, 104063. [[CrossRef](#)]
9. Hull, T. Counting Mountain-Valley Assignments for Flat Folds. *Ars Comb.* **2003**, *67*, 175–188.
10. Spong, M.W.; Hutchinson, S.; Vidyasagar, M. *Robot Modeling and Control*; John Wiley & Sons: Hoboken, NJ, USA, 2006.
11. Pratihar, D.K. *Fundamentals of Robotics: Manipulators, Wheeled and Legged Robots*; Alpha Science International Ltd.: Oxford, UK, 2017.
12. Zhang, Y.; Han, H.; Zhang, H.; Xu, Z.; Xiong, Y.; Han, K.; Li, Y. Acceleration analysis of 6-RR-RP-RR parallel manipulator with offset hinges by means of a hybrid method. *Mech. Mach. Theory* **2022**, *169*, 104661. [[CrossRef](#)]
13. Denavit, J.; Hartenberg, R.S. A Kinematic Notation for Lower-Pair Mechanisms Based on Matrices. *ASME J. Appl. Mech.* **1955**, *22*, 215–221. [[CrossRef](#)]

Disclaimer/Publisher’s Note: The statements, opinions and data contained in all publications are solely those of the individual author(s) and contributor(s) and not of MDPI and/or the editor(s). MDPI and/or the editor(s) disclaim responsibility for any injury to people or property resulting from any ideas, methods, instructions or products referred to in the content.